Check for updates

The Meteoritical Society

Meteoritics & Planetary Science 1–12 (2024)
doi: 10.1111/maps.14133

Unusual sources of fossil micrometeorites deduced from relict chromite in the small size fraction in ~467 Ma old limestone

Philipp R. HECK[1,2]*, Birger SCHMITZ[1,3], Xenia RITTER[1], Surya S. ROUT[1,2], Noriko T. KITA[4], Céline DEFOUILLOY[5], Katarina KEATING[1,2], Kevin EISENSTEIN[1], and Fredrik TERFELT[3]

[1]Robert A. Pritzker Center for Meteoritics and Polar Studies, Negaunee Integrative Research Center, Field Museum of Natural History, Chicago, Illinois, USA
[2]Department of the Geophysical Sciences, University of Chicago, Chicago, Illinois, USA
[3]Astrogeobiology Laboratory, Department of Physics, Lund University, Lund, Sweden
[4]WiscSIMS, Department of Geoscience, University of Wisconsin, Madison, Wisconsin, USA
[5]Cameca, Gennevilliers, France
Homi Bhabha National Institute, Training School Complex, Anushaktinagar, Mumbai 400094, India
School of Earth and Planetary Sciences, National Institute of Science Education and Research, Jatani, Khordha 752050, Odisha, India
***Correspondence**
Philipp R. Heck, Robert A. Pritzker Center for Meteoritics and Polar Studies, Negaunee Integrative Research Center, Field Museum of Natural History, 1400 S DuSable Lake Shore Dr, Chicago, IL 60614, USA.
Email: prheck@fieldmuseum.org

(Received 25 July 2023; revision accepted 21 December 2023)

ABSTRACT–Extraterrestrial chrome spinel and chromite extracted from the sedimentary rock record are relicts from coarse micrometeorites and rarely meteorites. They are studied to reconstruct the paleoflux of meteorites to the Earth and the collisional history of the asteroid belt. Minor element concentrations of Ti and V, and oxygen isotopic compositions of these relict minerals were used to classify the meteorite type they stem from, and thus to determine the relative meteorite group abundances through time. While coarse sediment-dispersed extraterrestrial chrome-spinel (SEC) grains from ordinary chondrites dominate through the studied time windows in the Phanerozoic, there are exceptions: We have shown that ~467 Ma ago, 1 Ma before the breakup of the L chondrite parent body (LCPB), more than half of the largest (>63 μm diameter) grains were achondritic and originated from differentiated asteroids in contrast to ordinary chondrites which dominated the meteorite flux throughout most of the past 500 Ma. Here, we present a new data set of oxygen isotopic compositions and elemental compositions of 136 grains of a smaller size fraction (32–63 μm) in ~467 Ma old pre-LCPB limestone from the Lynna River section in western Russia, that was previously studied by elemental analysis. Our study constitutes the most comprehensive oxygen isotopic data set of sediment-dispersed extraterrestrial chrome spinel to date. We also introduce a Raman spectroscopy-based method to identify SEC grains and distinguish them from terrestrial chrome spinel with ~97% reliability. We calibrated the Raman method with the established approach using titanium and vanadium concentrations and oxygen isotopic compositions. We find that ordinary chondrites are approximately three times more abundant in the 32–63 μm fraction than achondrites. While abundances of achondrites compared to ordinary chondrites are lower in the 32–63 μm size fraction than in the >63 μm one, achondrites are approximately three times more abundant in the 32–62 μm fraction than they are in the present flux. We find that the sources of SEC grains vary for different grain sizes, mainly as a result of parent body thermal metamorphism. We conclude that the meteorite flux composition ~467 Ma ago ~1 Ma before the breakup of the LCPB was fundamentally different from today and from other time windows studied in the

© 2024 The Authors. *Meteoritics & Planetary Science* published by Wiley Periodicals LLC on behalf of The Meteoritical Society.
This is an open access article under the terms of the Creative Commons Attribution License, which permits use, distribution and reproduction in any medium, provided the original work is properly cited.

Phanerozoic, but that in contrast to the large size fraction ordinary chondrites dominated the flux in the small size fraction. The high abundance of ordinary chondrites in the studied samples is consistent with the findings based on coarse extraterrestrial chrome-spinel from other time windows.

INTRODUCTION

Fossil relict micrometeorites recovered from marine sedimentary rock are useful to document changes in the sources and the flux of extraterrestrial materials to the Earth (Heck et al., 2017; Liao & Schmitz, 2023; Martin et al., 2018; Schmitz, 2013; Schmitz et al., 2017; Terfelt & Schmitz, 2021). While sediment diagenesis results in complete alteration of most phases, chromite and chrome spinel are durable and can retain their original structural, chemical, and isotopic composition. Up to now, classification was achieved by grouping grains by their major and minor elemental concentrations, notably of TiO_2 and V_2O_3, and by their oxygen isotopic compositions. Most previous work focused on fossil meteorites and micrometeorites recovered from sediments deposited immediately after the L chondrite parent body (LCPB) breakup ~466 Ma ago, the only documented time window with a record of a massively increased meteorite flux, by about two orders of magnitudes, for a duration of at least 1 Ma (Häggström & Schmitz, 2007; Heck et al., 2008, 2010, 2016; Schmitz et al., 2001, 2003, 2014, 2016; Schmitz, Farley, et al., 2019). One of our previous studies showed that 99% of the coarse (>63 μm) extraterrestrial chromite and chrome spinel are fragments generated in the LCPB (Heck et al., 2016). Only one meteorite in the L-chondrite-rich limestone sections deposited 1–2 Ma after the LCPB was classified as an ungrouped achondrite (Rout et al., 2018; Schmitz et al., 2014, 2016) and <1% of the micrometeorites were likely H chondritic (Heck et al., 2016). Subsequently, we have started to investigate the sources of extraterrestrial matter about 1 Ma years before the LCPB with oxygen isotopes (Heck et al., 2017). Based on analyses of sediment-dispersed extraterrestrial coarse chrome spinel and chromite (SEC) grains >63 μm in diameter from the GAP7 bed in the Lynna River section in Russia, we have shown that, at that time, an unusually large fraction of coarse micrometeorites were from the howardite–eucrite–diogenite (HED) clan and from primitive and ungrouped achondrites originating from differentiated and partially differentiated asteroids. We also found that the three ordinary chondrite groups, H, L, and LL, occurred in similar proportions. We attributed the abundance of a particular group to distinct collisional events in the asteroid belt that generated fragments that ended up on Earth. Following work has also shown that the relative abundances of different meteorite groups varied in the Cretaceous (Schmitz et al., 2017), Devonian (Schmitz, Feist, et al., 2019), the Silurian (Martin et al., 2018), and the Cambrian (Terfelt & Schmitz, 2021), but that during most studied time windows, ordinary chondrites dominated the coarse chromite-bearing extraterrestrial material flux to the Earth. A recent study of the smaller size fraction (32–63 μm) SEC grains (~900 grains) from the ~467 Ma pre-LCPB breakup time window based on classifications using elemental compositions that also includes 651 grains from the same sediment bed and time window determined an overabundance of ordinary chondrites over achondrites (Liao & Schmitz, 2023).

Here, we present oxygen isotopic *and* elemental microanalyses of 136 chrome-spinel grains from a subset of the same size fraction from the ~467 Ma old time interval as studied by Liao and Schmitz (2023). This is the smaller size fraction (32–63 μm) compared to our previous study (Heck et al., 2017) which focused on 46 grains larger than 63 μm but a larger sample set from the GAP7 bed of the Lynna River section in Russia. Our primary motivation for the present study was to investigate how the elemental *and* oxygen isotopic composition of the smaller size fraction and hence the relative type abundance differ from the larger one that was previously studied at a more granular level, and to search for new sources of micrometeorites. We also include new data from five grains >63 μm from the same time interval that we obtained. Additionally, we present our new classification method of extraterrestrial chrome-spinel grains based on Raman spectroscopy.

SAMPLES AND METHODS

Samples

We randomly selected 183 chrome-spinel grains from the 651 grains used in the Liao and Schmitz (2023) study from the Middle Ordovician ~467 Ma old limestone in the Lynna River section near St. Petersburg, Russia (Lindskog et al., 2012) that were recovered by acid dissolution and sieving of the acid residue. The grains were handpicked under a binocular microscope, mounted on carbon tape for identification with scanning electron microscopy and energy-dispersive X-ray spectroscopy (SEM/EDS), and then imaged and quantitatively analyzed for major and minor elements with SEM/EDS and electron probe microanalyzer and wavelength-

19455100, 0, Downloaded from https://onlinelibrary.wiley.com/doi/10.1111/maps.14133 by Readcube (Labtiva Inc.), Wiley Online Library on [03/02/2024]. See the Terms and Conditions (https://onlinelibrary.wiley.com/terms-and-conditions) on Wiley Online Library for rules of use; OA articles are governed by the applicable Creative Commons License

dispersive X-ray spectroscopy (EPMA/WDS) in polished epoxy mounts (Liao & Schmitz, 2023).

The sampled subsection GAP7 was deposited ~1 Ma prior the LCPB to avoid the abundant L chondrite fragments produced during the breakup event.

Identification and Classification

For the classification solely based on SEC elemental composition, we use the nomenclature by Terfelt and Schmitz (2021). They define equilibrated ordinary chondritic chrome-spinel grains as "EC" (not to be confused with enstatite chondrites), other chrome-spinel as "OtC" and "OtC" grains with > 0.55 wt% V_2O_3 as OtC-V grains. Compositional ranges and likely meteorite sources are given in Table S1. This classification can distinguish between grains from equilibrated ordinary chondrites and other meteorites, and among equilibrated ordinary chondrites distinguish between the groups H, L, and LL chondrites. The system was initially calibrated with oxygen isotopes (Heck et al., 2010). The classification of chrome-spinel grains from other meteorites requires the analyses of oxygen isotopes in individual grains (Heck et al., 2017). We used the WiscSIMS Cameca IMS-1280 ion microprobe/secondary ion microprobe spectrometry (SIMS) to analyze three oxygen isotopes using the analytical protocols similar to Heck et al. (2010) and Kita et al. (2010) and the instrumental bias corrections using a set of chromite and spinel standards (Heck et al., 2010). We used a 13 μm × 10 μm beam size (2.4 nA) with a typical secondary $^{16}O^-$ intensity of 4.5×10^9 cps. The external reproducibilities of the UWCr-3 bracketing standard were 0.28‰, 0.25‰, and 0.23‰ for $\delta^{18}O$, $\delta^{17}O$, and $\Delta^{17}O$, respectively. We corrected the ^{17}O signal for a $^{16}O^1H$ hydride peak tailing interference, which was relatively higher during the SIMS session (26 ppm) compared to previous studies (≤10 ppm) due to a slightly elevated pressure at the detection chamber. We analyzed 183 grains (195 spots) for oxygen isotopes but rejected 42 analyses due to large $^{16}O^1H$ corrections (>0.5‰), so we ended up with useful 148 O-isotope data sets for 141 grains. The rejection rate of 24% was due to a combination of the OH correction factor (26 ppm) and the high OH/O ratios of the chrome-spinel grains in this study.

The combined approach by using $\Delta^{17}O$ values and TiO_2 and V_2O_3 concentrations allows a more granular classification of grains (Heck et al., 2017 and Table S2) than solely with elemental concentrations. For example, with this method, some grains can be classified unambiguously as HED type, carbonaceous chondrites, and R chondrites. Also, any Martian chromites would be detectable with oxygen isotopes. Some ambiguity remains for low-TiO_2 grains (<2 wt%) with $\Delta^{17}O$ values in the HED range around −0.5‰ that can be either HED type, brachinites, or ungrouped achondrites. While SIMS analysis combined with EDS/WDS allows for a more granular classification, it is more time-consuming and expensive than EDS/WDS analysis alone. EDS/WDS analysis is quicker and more cost-effective than SIMS and allows a larger number of samples to be analyzed for better type abundance statistics but at a less granular level. Thus, the combined oxygen isotopes and elemental concentration approach provides a powerful method that is practical for smaller sample sets up to about 200 grains.

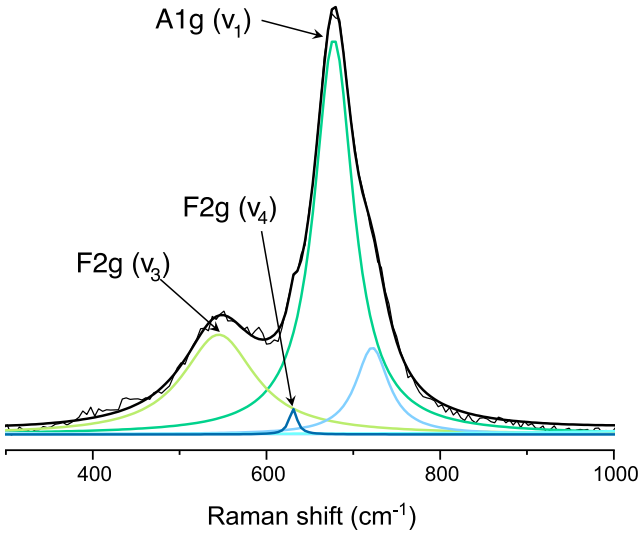

FIGURE 1. Raman spectrum of a representative chrome spinel grain from this study.

After post-SIMS SEM imaging, we used Raman spectroscopy to analyze the polished grains to screen for the possible presence of high-pressure polymorphs generated by impacts (Rout et al., 2017). For this study, we used the Field Museum's WITec alpha 300R Raman spectroscopy system equipped with a green laser of 532 nm. For spot analyses, we used ~10 mW laser power, 20–40s integration per spot, 600 or 1800 g mm^{-1} grating, and 50× magnification. Spectral stability was monitored by analyzing an Si wafer in each session and recording the position of the first-order Si peak. Peak shifts were corrected by adding or subtracting the observed deviation of the measured position of the first-order Si peak from its nominal position at 520 cm^{-1}. Subsequent spectral analysis was carried out using Fityk (Wojdyr, 2010) to model two to three individual Raman modes (A1g(v1), F2g(v4), F2g(v3) after Wang et al., 2004) contributions by fitting Lorentzian functions (Figure 1).

Interpretation of Raman Spectra

We applied Raman spectroscopy to identify any previously unknown correlations between signature vibrational stretching and the SEC origin in accordance with its chemical composition.

19455100, 0, Downloaded from https://onlinelibrary.wiley.com/doi/10.1111/maps.14133 by Readcube (Labtiva Inc.), Wiley Online Library on [03/02/2024]. See the Terms and Conditions (https://onlinelibrary.wiley.com/terms-and-conditions) on Wiley Online Library for rules of use; OA articles are governed by the applicable Creative Commons License

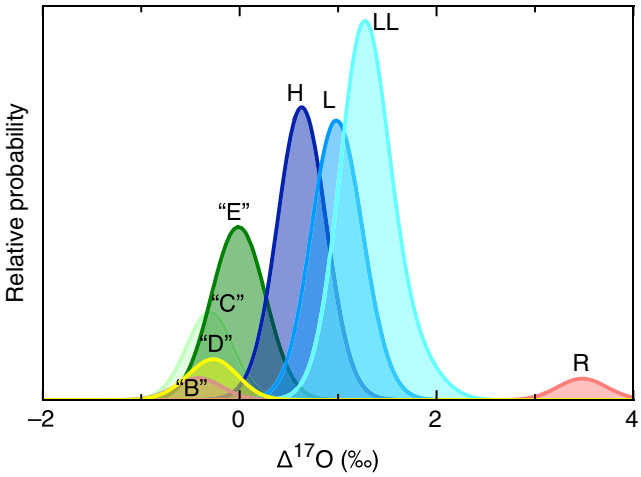

FIGURE 2. Probability density functions (PDFs) of $\Delta^{17}O$ values of the different micrometeorite categories. Summed PDFs from grouped data of individual chrome-spinel grains labelled with the categories from Heck et al. (2017) and H, L, LL, and R chondrites.

Factor group analyses (Tuschel, 2015) suggested five Raman-active vibrational modes for normal spinel structure in the Fd3m space group: A1g (v_1) + Eg (v_2) + 3F2g (v_3, v_4, translation Chopelas & Hofmeister, 1991). The primitive unit cell consists of two formula units $[^{IV}(Fe^{2+}, Mg^{2+})^{VI}(Cr^{3+}, Fe^{3+}, Al^{3+})_2O_4]$ with a cubic close-packed array of oxygen atoms, trivalent cations occupying half of the octahedral interstices, and divalent cations occupying one-eighth of the tetrahedral interstices. Chromite and chrome-spinel Raman spectra in this study are characterized by a dominant A1g (v1) peak at ~670–725 cm^{-1} with a shoulder at ~650 cm^{-1} (F2g, v_4), caused by bonds in the $(Cr^{3+}, Fe^{3+}, Al^{3+})O_6$ octahedra (Malézieux & Piriou, 1988; Wang et al., 2004). Figure 1 shows that the main A1g peak can be fitted by two to three underlying vibration modes; however, the shoulder on the high shift side is not always visible.

The low-intensity and broad peak at ~530–595 cm^{-1} were identified in this study as F2g (v_3) mode (Figure 1), which is in agreement with the occurrence reported at 600 cm^{-1} by Wang et al. (2004) but not with Reddy and Frost (2005), who reported the F2g (v_3) mode at a Raman shift of 218 cm^{-1}.

RESULTS AND DISCUSSION

Classification and Type Abundances

We have analyzed a total of 183 grains and classified 141 of them with oxygen isotopes and elemental compositions, and the remaining only with elemental compositions.

Results are displayed as probability density function plots assigned to the different categories (Figure 2) and in the $\Delta^{17}O$ and TiO_2 compositional space (Figure 3). We grouped the grains into different categories as defined in Heck et al. (2017). The results and categories are given in Tables S2 and S3, with data shown in Figures 2 and 3 and a full data set provided in the Electronic Supplement. From the 141 grains that we classified with a combination of elemental analyses and oxygen isotopes, 94 are consistent with extraterrestrial compositions. Of the 136 from the small size fraction, 72 are from ordinary chondrites, with 19 H chondrites, 31 L chondrites, and 22 LL chondrites. The H:L:LL abundance ratios normalized to L chondrites are 0.6: 1.0: 0.7 and show a lower relative abundance of LL chondrite than in the larger (>63 μm) size fraction where the ordinary chondrite group abundance ratios are 0.6: 1.0: 1.0. We find 21 grains from achondrites which correspond to an achondrite to ordinary chondrite ratio of about 1:3. There may be up to 18 HED grains based on $\Delta^{17}O$ and TiO_2 values (groups C, D, E); however, nine of these grains have low TiO_2 values and could be also from Brachinites or ungrouped achondrites (Figure 3). Thus, the seven grains with $\Delta^{17}O$ values in the HED field and TiO_2 values >2 wt% (the two group D grains and five group E grains) can be classified as HED grains (Figure 3). This leaves 12 grains assigned to primitive or ungrouped achondrites based on oxygen isotopes and elemental compositions (groups A, B, C, E). In addition to ordinary chondrites and achondrites, we found one R chondritic grain, something that has not been observed before in the fossil micrometeorite record.

The five randomly picked larger grains (>63 μm) fall into categories B, C, D as well two terrestrial grains ("F"). Interestingly, none of them has an ordinary chondritic composition.

None of the analyzed grains in either size fraction exhibits compositional zoning, confirming chemical homogeneity due to growth and full equilibration during thermal metamorphism.

While there is some agreement in the classification determined with the combined oxygen isotope/elemental concentration method compared to the method using only elemental concentrations, the latter tends to undercount extraterrestrial grains as it classifies some primitive and ungrouped achondrite grains with nonterrestrial D17O values as possibly terrestrial ("OtC" in Terfelt & Schmitz, 2021). Also, our data show that, without oxygen isotopes, ordinary chondritic grains are undercounted as some are classified as nonordinary chondritic ("OtC-V" in Terfelt & Schmitz, 2021). Nevertheless, the method without oxygen isotopes remains valuable as it still captures most ordinary chondrite grains and has the potential to yield larger data sets that result in smaller statistical errors on type abundances compared to the smaller data sets for which oxygen isotope analysis is feasible.

19455100, 0, Downloaded from https://onlinelibrary.wiley.com/doi/10.1111/maps.14133 by Readcube (Labtiva Inc.), Wiley Online Library on [03/02/2024]. See the Terms and Conditions (https://onlinelibrary.wiley.com/terms-and-conditions) on Wiley Online Library for rules of use; OA articles are governed by the applicable Creative Commons License

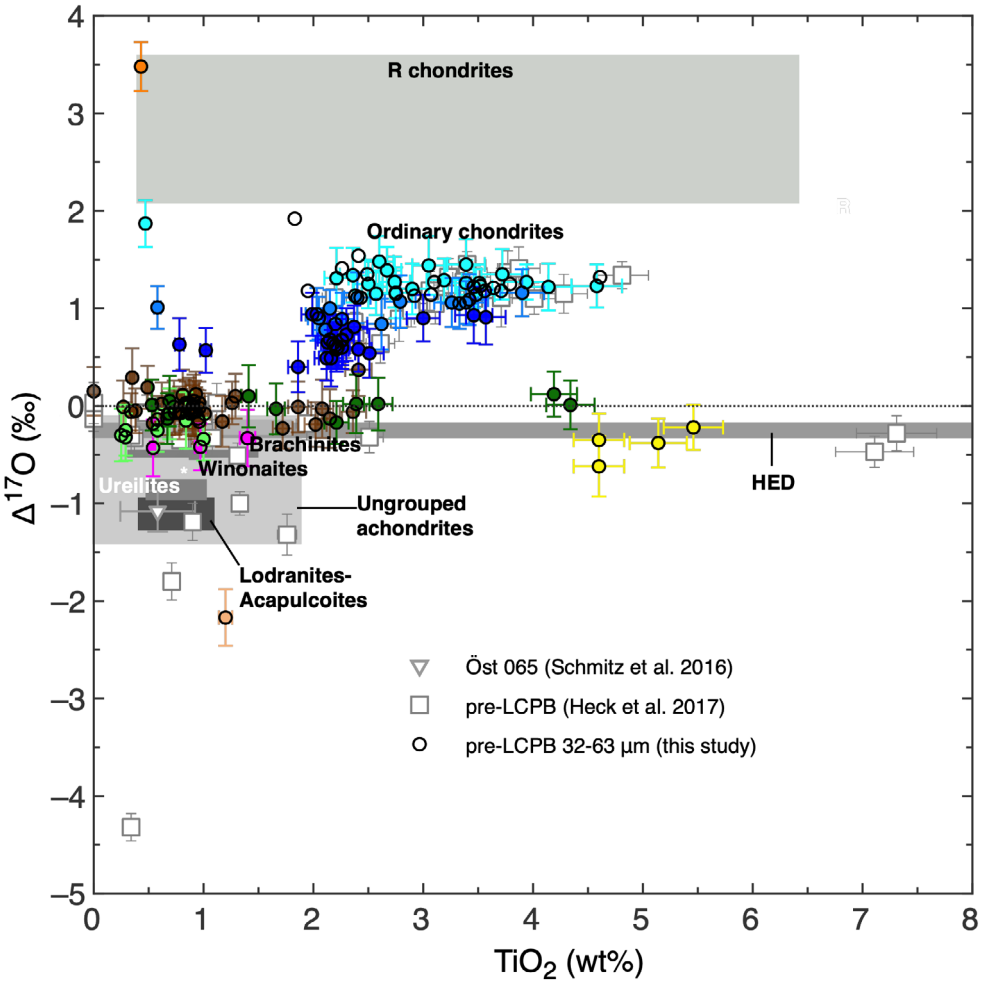

FIGURE 3. Oxygen isotopic composition and TiO_2 concentrations are routinely used to classify extraterrestrial relict chrome-spinel grains found in sedimentary rock. Color coding of data points corresponds to categories shown in Figure 2.

Classification with Raman Spectroscopy

We cross-correlated fitted peak positions of the three distinct modes (v_1, v_3, v_4) measured on chrome spinel of different groups. A correlation between terrestrial and extraterrestrial as a function of wave number is apparent for all three modes (shown for the A1g and v_4 peaks in Figure 4). Thus, we define the category for terrestrial chromites to begin above wave numbers of 683, ~557, and 644 cm^{-1} for v_1, v_3, and v_4, respectively. The category for extraterrestrial chromites is defined as wave numbers below 678, 547, and 634 cm^{-1} for peak positions of v_1, v_3, and v_4, respectively.

The position of the A1g (v1) mode is known to be strongly correlated with compositional changes: It is known to move toward higher wave numbers with increasing Al^{3+} and decreasing Cr^{3+} in the sample due to cation substitution between Cr^{3+}, Fe^{3+}, and Al^{3+} on the octahedral sites forming a solid solution (e.g., Malézieux & Piriou, 1988; Wang et al., 2004). Figure S2 shows the correlation $(Cr^{3+} + Fe^{3+})/(Cr^{3+} + Fe^{3+} + Al^{3+})$ versus the A1g (v1) mode (Malézieux & Piriou, 1988) measured on the grains from this study to describe the Cr^{3+} and Fe^{3+} occupancy on the octahedral sites. The results show a strong agreement with literature data (Malézieux & Piriou, 1988; Naveen et al., 2019; Wang et al., 2004) and thus confirms the known trend.

We show that the A1g peak position can be used as an identification tool to distinguish between terrestrial and extraterrestrial chromite grains. Such a distinction is particularly prominent when plotting the A1g peak position; $\Delta^{17}O$ values; and the TiO_2, V_2O_3, and Al_2O_3 concentrations (Figure 5). In our study, grains with A1g peaks <683 cm^{-1} are extraterrestrial, as defined as any category other than "F," with a confidence of ~97%. In our data set, we like to highlight one outlier, sample 218_gr27 (shown in Figure 5 as an open circle centered on a filled circle) which is terrestrial based on its $\Delta^{17}O$

19455100, 0, Downloaded from https://onlinelibrary.wiley.com/doi/10.1111/maps.14133 by Readcube (Labtiva Inc.), Wiley Online Library on [03/02/2024]. See the Terms and Conditions (https://onlinelibrary.wiley.com/terms-and-conditions) on Wiley Online Library for rules of use; OA articles are governed by the applicable Creative Commons License

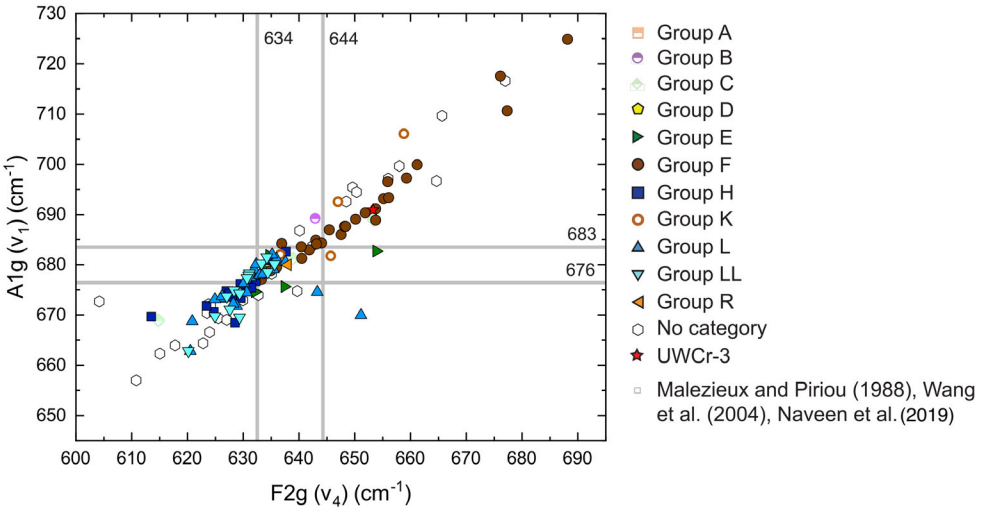

FIGURE 4. Cross-correlation between the A1g (v1) and F2g (v4) Raman peaks (modes).

(0.01 ± 0.26‰) and $\delta^{18}O$ (3.75 ± 0.26‰) values and the Raman A1g peak position (706 cm^{-1}), while its high TiO_2 (4.34 ± 0.22 wt%) and V_2O_3 (0.54 ± 0.03 wt%) concentrations alone would have suggested it is extraterrestrial. The Raman spectra shown in Figure S3 depict the differences between terrestrial and extraterrestrial chromites. The terrestrial chromites have spectra with broader peak shapes, as opposed to ordinary chondrites and achondrites. A broad A1g peak shape may arise from low crystallinity and stronger terrestrial weathering. The broad shape of the F2g (v_3) peak is due to increased Al_2O_3 content in comparison to endmember chromites, which show several distinct low-intensity peaks between ~500 and ~600 cm^{-1} (Naveen et al., 2019; Wang et al., 2004).

Figure S4 shows the peak position of A1g v1 mode and major element compositions (MgO, Al_2O_3, TiO_2, V_2O_3, Cr_2O_3, MnO, FeO, ZnO) in wt%. The distinction between terrestrial and extraterrestrial can be observed particularly well for Al_2O_3 and V_2O_3.

We have screened all SEC grains and its olivine inclusions, found in six grains, for high-pressure polymorphs which would distinguish themselves by differences in Raman spectra (Rout et al., 2017). We did not find any high-pressure polymorph in the analyzed samples.

DISCUSSION

The Effect of Thermal Metamorphism on Grain Size

Abundances of different types of coarse micrometeorites in the studied time window were markedly different than today with a higher abundance of achondrites. We observe that the relative abundance of achondritic grains in the smaller size fraction is lower (achondrite–ordinary chondrite ratio of about 1:3) than in the larger size fraction (achondrite–ordinary chondrite ratio of 1:<1.3; Heck et al., 2017). This is expected and can be explained by larger chrome-spinel grains being products of high degrees of thermal processing in achondrite parent bodies compared to the thermal metamorphism that occurred in ordinary chondrite parent bodies. While Bridges et al. (2007) found a positive correlation between maximum average diameters of chromite grains and the degree of thermal metamorphism described as increased petrographic type in ordinary chondrites, higher degrees of thermal metamorphism in achondrites result in a higher fraction of large grains than due to thermal metamorphism in ordinary chondrite parent bodies. This would explain that achondrites in the large grain size fraction are more abundant than in the smaller grain size fraction studied.

Asteroidal Sources: HED Meteorites

In the small size fraction analyzed in this study, the relative abundance of grains of HED achondritic type to ordinary chondrites was similar to today. The larger abundance of HED grains in the larger size fraction in Heck et al. (2017) was attributed to the higher flux of HED ejecta from the decaying impact curve from the Rheasilvia basin forming event on Vesta ~1 Ga ago. We note that the age of the Rheasilvia basin is debated: while the ~1 Ga age was initially based on dynamical simulations and Dawn observations (Marchi et al., 2012) and dynamical ages of the Vesta asteroid family (Marzari et al., 1996, 1999; Milani et al., 2014), a crater-counting age based on a scaled lunar chronology estimates the basin to have formed ~3.5 Ga ago (Schmedemann et al., 2014). A similarly old age was also inferred from ^{40}Ar-^{39}Ar

19455100, 0, Downloaded from https://onlinelibrary.wiley.com/doi/10.1111/maps.14133 by Readcube (Labtiva Inc.), Wiley Online Library on [03/02/2024]. See the Terms and Conditions (https://onlinelibrary.wiley.com/terms-and-conditions) on Wiley Online Library for rules of use; OA articles are governed by the applicable Creative Commons License

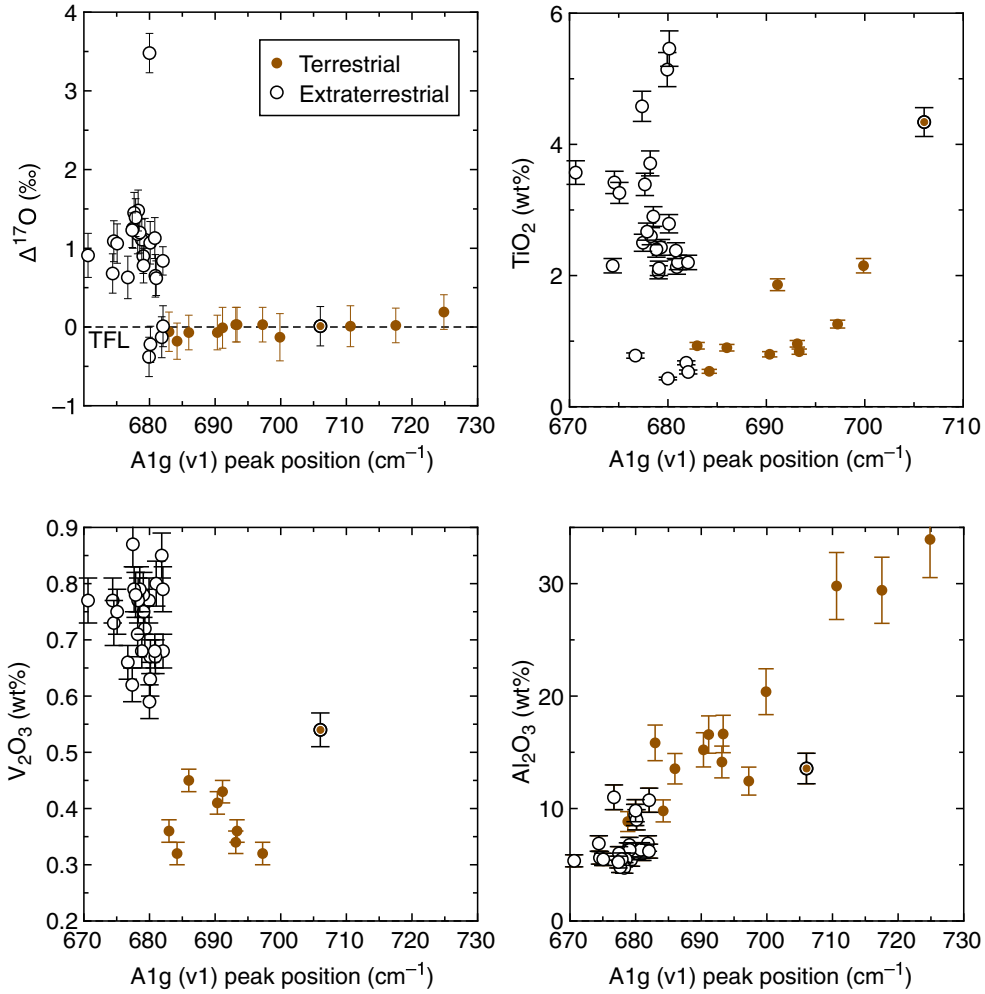

FIGURE 5. Cross plots between prominent Raman peak A1g, $\Delta^{17}O$ and diagnostic minor element compositions of chrome-spinels. Extraterrestrial grains (all categories other than "F") can be distinguished from terrestrial grains with a A1g peak position >683 cm^{-1} (classified as category "F"). Only datapoints with OH corrections <0.5‰ are shown here. Please note that sample 218_gr27 is an outlier (filled and open circle symbol) as it is terrestrial based on its oxygen isotopic composition and the Raman A1g peak position, whereas its TiO_2 and V_2O_3 would suggest it is extraterrestrial.

dating of eucrites which were interpreted as samples of rubble pile asteroids that formed from Rheasilvia ejecta (Jourdan et al., 2020; Kennedy et al., 2019). However, recent work by Schenk et al. (2022) carefully reexamined the age of the basin and gives a young Rheasilvia event a higher probability than previous studies. That work is based on new crater counting statistics not relying on scaled lunar data along with structural geology observations with NASA's Dawn spacecraft data (Roig & Nesvorný, 2020; Schenk et al., 2022) and sets the Rheasilvia formation event to 0.8–0.9 Ga. We note that a dynamical study based on debiased astronomical observations of asteroids found an age of the Vesta family of >1.3 ± 0.1 Ga (Dermott et al., 2021) that is >400 Ma older than the Schenk et al. (2022) age. The Dermott et al. (2021) age is consistent with the ~1.4 Ga ^{40}Ar-^{39}Ar ages of feldspars close to veins from brecciated howardite Kapoeta (Lindsay et al., 2015). Only one HED meteorite, Yamato-74097, has a bulk ^{40}Ar-^{39}Ar age between 1.0 and 1.3 Ga (Kaneoka et al., 1979). The old bulk ^{40}Ar ages of many HED meteorites determined in several studies (Bogard, 2011; Bogard & Garrison, 2003; Cohen, 2013; Jourdan et al., 2020; Kennedy et al., 2019) indicate that their radiogenic Ar clocks did not get reset during the Rheasilvia event, but do not preclude that meteorites were ejected at that time. The lack of impact melt deposits in the Rheasilvia basin indicates that the impact did not produce large amounts of melt and was of normal velocity (Marchi et al., 2012). Immediate ejection of fragments into space resulted in their rapid cooling that prevented significant Ar loss through diffusion (Schenk et al., 2022). Argon loss in bulk rock samples is facilitated by slower cooling (Bogard & Garrison, 2003) over >10^4 years, something that could have occurred in rocks beneath craters.

19455100, 0, Downloaded from https://onlinelibrary.wiley.com/doi/10.1111/maps.14133 by Readcube (Labtiva Inc.), Wiley Online Library on [03/02/2024]. See the Terms and Conditions (https://onlinelibrary.wiley.com/terms-and-conditions) on Wiley Online Library for rules of use; OA articles are governed by the applicable Creative Commons License

Thus, current evidence can account for both the young and old Ar ages of HED samples and points to a young age for Rheasilvia. While the Vestoids and HED meteorites were likely formed in the Rheasilvia event, the chrome-spinel samples do not allow us to determine the rock type—if the relict minerals were parts of breccia or unbrecciated rocks, thus making it impossible to assign them to Vesta or Vesta-like rubble pile asteroids. In either case, the remarkably higher abundance of HED micrometeorites with large chrome-spinel grains preserved in Ordovician sedimentary rocks requires that a major impact event on Vesta or a Vesta-like asteroid released large amounts of ejecta before 467 Ma ago. The two earlier time windows that were studied are in the Late Cambrian around ~500–499 Ma and ~503–502 Ma did not reveal an increased fraction of nonordinary chondrites (Terfelt & Schmitz, 2021) compared to the GAP7 time window at 467–466 Ma in the Ordovician studied here. In the Cambrian study that relied on elemental analyses, any HED grains would fall into the "OtC-V" category (meteorites other than equilibrated ordinary chondrites). The ratio of equilibrated ordinary chondrites to "OtC-V" for large grains (>63 μm) in the older Cambrian window is 1.2 (Terfelt & Schmitz, 2021) which is identical with the GAP7 ratio of 1.1–1.3 (Heck et al., 2017; Schmitz et al., 2017; Schmitz, Farley, et al., 2019; Terfelt & Schmitz, 2021) indicating the same high abundance of large grains from other meteorites, including HEDs and presumably primitive and ungrouped achondrites. However, the ratio in the younger Cambrian window is 3.7 and for the smaller grains (32–63 μm) in both the young and old Cambrian windows is 3.6 and 3.1, respectively. This is due to a—currently unexplained—higher flux of equilibrated H chondrites in the Cambrian. Thus, despite the lower *relative* abundance, the flux of HED and other achondrites was already very high, similar to the GAP7 time window. Hence, the HED meteorites and micrometeorites that arrived on Earth between 503 and 466 Ma were ejected from members of the Vesta family in secondary impacts on the order of tens of millions of years before, as this is their typical delivery time from the asteroid belt to the Earth (Herzog & Caffee, 2013), at least ~400 Ma after the Rheasilvia event.

The L Chondrites

The scarcity of HED meteorites with degassing ages corresponding to the Vesta family forming event stands in contrast to the large fraction of L chondrites with Ar-Ar ages requiring full degassing during the LCPB ~466 Ma but can be explained with a lack of an (identifiable) asteroid family that formed during the LCPB breakup the initial Gefion family hypothesis (Nesvorný et al., 2009) is being questioned since the discovery of H chondrites and possibly achondrites in this family (McGraw et al., 2018; Vernazza et al., 2014). Previous studies have shown, starting with the cosmic ray exposure ages of fossil meteorites from deposits that formed shortly after the LCPB breakup (Heck et al., 2004) and subsequent physical calculations (Nesvorný et al., 2007, 2009), that the breakup event must have happened close to an orbital resonance and that fragments were directly injected into it. Exposure ages of the fossil meteorites are so short that the breakup must have happened close to an orbital mean motion resonance; otherwise, transfer times would be much longer. While there seems no consensus yet on which orbital resonance was responsible for delivering the LCPB fragments to the Earth, these studies discuss the 3:1, nu6, and 5:2 resonances as possible sources, with the latest study on this topic (Nesvorný et al., 2009) giving preference to the 5:2 resonance. A high-velocity impact that caused the LCPB would explain the significant heating that caused radiogenic Ar loss in those rocks that remained buried and cooled slowly but would have also resulted in fast ejecta of other fragments into an orbital resonance that lead to extremely short cosmic ray exposure ages (Heck et al., 2004, 2008; Nesvorný et al., 2007, 2009). To explain the shortest exposure ages determined in fossil L chondrites, unusually fast ejection velocities are needed (Nesvorný et al., 2007, 2009). The fact that the LCPB resulted in a large fraction of rock fragments that cooled slowly indicates that the asteroid may have reaccreted to form a rubble pile rather than an asteroid family, which is consistent with recent work that lacks observational evidence for an L chondrite asteroid family related to the LCPB. The L chondrites found in the present study were obviously released from their parent body before the breakup of the LCPB. It is remarkable that, at that time, L chondrites already dominated the ordinary chondrite flux but were close in type abundance as the H and LL chondrites (0.6:1.0:0.7; H:L:LL).

Asteroidal Sources: LL Chondrites

The abundance of LL chondrites relative to all ordinary chondrite groups was 31%, which is approximately three times more abundant compared to the 11% today. Heck et al. (2017) suggested the higher abundance of LL chondrites in the GAP7 sample is a result of the GAP7 samples formed closer in time to proposed massive LL chondrite release in the Flora family formation event ~1 Ga ago. The LL chondrites were likely released in secondary impacts onto an LL chondrite parent body, similar to the Morokweng LL chondrite (625 ± 163 Ma; Jourdan et al., 2010) while the dynamical age of the Flora asteroid family is 950 + 200/−170 Myr (Dykhuis et al., 2014). That implies that the LL chondrite flux was variable, overprinted on a decaying flux curve, rather than a smooth decay function.

19455100, 0, Downloaded from https://onlinelibrary.wiley.com/doi/10.1111/maps.14133 by Readcube (Labtiva Inc.), Wiley Online Library on [03/02/2024]. See the Terms and Conditions (https://onlinelibrary.wiley.com/terms-and-conditions) on Wiley Online Library for rules of use; OA articles are governed by the applicable Creative Commons License

In the absence of other explanations to date, this still seems to be a plausible scenario.

Asteroid Sources: Other Achondrites and R Chondrites

The type abundance of primitive and ungrouped achondrites in our Ordovician time window (GAP7) was at least three times higher than today, measured as the achondrite to chondrite ratio (but the sources and events that ejected primitive and ungrouped achondrites remain unknown but must be the result of a collisional event on their [partially] differentiated parent asteroids). Asteroids with high orthopyroxene and low olivine contents, compositions consistent with primitive achondrites, were found spectroscopically in the asteroid belt, associated with the Gefion and Hungaria families (Lucas et al., 2017; McGraw et al., 2018). However, the observational sample is still small, and it cannot be ruled out that these primitive achondritic asteroid samples are not genetically associated with the families where they were found in McGraw et al. (2018). Thus, currently the primitive achondrites found in our GAP7 samples cannot be linked with confidence to an asteroid family.

The rare chrome-spinel grains that have positive $\delta^{17}O$ and $\delta^{18}O$ values are on or close to the 1:1 line in three oxygen isotopic space and have low TiO_2 concentrations (<0.5 wt%). Such a composition is not observed in chrome spinel from any known meteorite group; however, it has been observed in hydrous alteration phases such as magnetite in unequilibrated chondrites and in recent micrometeorites. In contrast to magnetite, chrome spinel is a product of thermal metamorphism and should not be affected by aqueous alteration. Similar compositions were also found in comet dust crater residue from the Stardust mission but are likely also unrelated due to the absence of coarse chromite in Wild 2 comet dust. A small fraction of recently fallen Antarctic micrometeorites revealed bulk oxygen isotopic compositions that are similar to our unusual samples and are possibly attributed to R chondrites (Group IV in Suavet et al., 2010). The $\Delta^{17}O$ values of our samples are consistent with an R chondrite origin, the TiO_2 compositions (<0.5 wt%) are at the lower end of the range known for chrome spinel from R chondrites (Figure 3). Other ^{16}O-poor materials were found recently in micrometeorites and were related to CY chondrites (Suttle et al., 2020).

Implications for Our Knowledge of the Flux Composition Over Time

Terfelt and Schmitz (2021) argued that ordinary chondrites dominated the flux to the Earth of coarse chromite-bearing ET matter in the last 541 million years, the Phanerozoic Eon, based on a review of data from 15 time windows. However, significant variations in the flux of HED meteorites, other achondrites, and among the ordinary chondrite groups occurred, as discussed in Terfelt and Schmitz (2021), Heck et al. (2017), and in this study. Heck et al. (2017) and this study provide a granular view into the type abundances and sources of coarse chromite-bearing ET matter preserved on Earth at a level of detail that is not achievable by elemental classification methods alone. In the studied time window, achondrites dominated over ordinary chondrites in the largest size fraction (Heck et al., 2017) but not in the smaller size fraction (this study, Liao & Schmitz, 2023). A systematic study of different achondritic size fractions in the 15 and more time windows will reveal how ejecta from different sources vary over time and can serve as ground truth data for dynamical models of collisional dynamics in the asteroid belt and inner solar system in the Phanerozoic Eon. Little is known about the type abundances of the size fraction <32 μm in the Earth's sedimentary rock record, which includes unequilibrated meteorites including most carbonaceous chondrite, unequilibrated ordinary chondrites, and also achondrites. Identifying such grains is even more difficult and time-consuming because terrestrial grains dominate by orders of magnitude in that size fraction as they can be easily transported by marine currents and "dilution" of extraterrestrial matter is increasing with decreasing grain size.

CONCLUSIONS

Our study underlines the importance of distinguishing between different size fractions and demonstrates the benefits of using oxygen isotopic analyses of chrome-SEC for the classification of achondrites. We confirm that the composition of the micrometeorite flux ~467 Ma ago was fundamentally different than today with a high relative abundance of achondritic material. In particular, HED meteorites, primitive achondrites, and related ungrouped achondrites were almost ~3× more abundant than today. Ordinary chondrite groups occurred in different relative abundances than today while overall ordinary chondrites were more abundant in the smaller (32–63 μm) size fraction than in the one >63 μm. We found one rare R chondrite grain, the first found in a fossil micrometeorite collection.

We show that we can distinguish SEC grains from terrestrial chrome spinel with Raman spectroscopy in the Russian Lynna River section. In addition to oxygen isotopic compositions, TiO_2 and V_2O_3 concentrations, the Raman spectroscopy approach is an independent, cost-effective method to identify SEC and simultaneously screen them for high-pressure polymorphism. In our sample set, we did not find any high-pressure phases.

19455100, 0, Downloaded from https://onlinelibrary.wiley.com/doi/10.1111/maps.14133 by Readcube (Labtiva Inc.), Wiley Online Library on [03/02/2024]. See the Terms and Conditions (https://onlinelibrary.wiley.com/terms-and-conditions) on Wiley Online Library for rules of use; OA articles are governed by the applicable Creative Commons License

We confirm that individual impact events are responsible for the diversity of materials that arrive on Earth from space. Ejecta from such events typically get deposited on Earth on the order of typical cosmic ray exposure ages, dozens of million years after the event, unless fragments got directly injected into an orbital resonance, which is only known for after the LCPB breakup event. The origin of more abundant primitive and ungrouped achondrites remains a mystery. And finally, our results are consistent with Terfelt and Schmitz (2021) and Liao and Schmitz (2023) that, in the small size fraction, ordinary chondrites dominated the flux of chromite-bearing extraterrestrial matter to the Earth during the Phanerozoic.

Acknowledgments—The authors acknowledge funding from the TAWANI Foundation, the Negaunee Foundation, and the Field Museum's Science and Scholarship Funding Committee. WiscSIMS is partly supported by NSF (EAR-1658823). PRH thanks William Bottke and Simone Marchi for helpful discussions. The authors are grateful by the constructive reviews by Jemma Davidson and editor Donald Brownlee.

Conflict of Interest Statement—The authors declare no conflicts of interest.

Data Availability Statement—The data that support the findings of this study are available in the supplementary material of this article.

Editorial Handling—Dr. Donald E. Brownlee

REFERENCES

Bogard, D. D. 2011. K-Ar Ages of Meteorites: Clues to Parent-Body Thermal Histories. *Chemie der Erde* 71: 207–226.

Bogard, D. D., and Garrison, D. H. 2003. ^{39}Ar-^{40}Ar Ages of Eucrites and Thermal History of Asteroid 4 Vesta. *Meteoritics & Planetary Science* 38: 669–710.

Bridges, J. C., Schmitz, B., Hutchison, R., Greenwood, R. C., Tassinari, M., and Franchi, I. A. 2007. Petrographic Classification of Middle Ordovician Fossil Meteorites from Sweden. *Meteoritics & Planetary Science* 42: 1781–89.

Chopelas, A., and Hofmeister, A. M. 1991. Vibrational Spectroscopy of Aluminate Spinels at 1 atm and of $MgAl_2O_4$ to over 200 kbar. *Physics and Chemistry of Minerals* 18: 279–293.

Cohen, B. A. 2013. The Vestan Cataclysm: Impact-Melt Clasts in Howardites and the Bombardment History of 4 Vesta. *Meteoritics & Planetary Science* 48: 771–785.

Dermott, S. F., Li, D., Christou, A. A., Kehoe, T. J. J., Murray, C. D., and Robinson, J. M. 2021. Dynamical Evolution of the Inner Asteroid Belt. *Monthly Notices of the Royal Astronomical Society* 505: 1917–39.

Dykhuis, M. J., Molnar, L., Van Kooten, S. J., and Greenberg, R. 2014. Defining the Flora Family: Orbital Properties, Reflectance Properties and Age. *Icarus* 243: 111–128.

Häggström, T., and Schmitz, B. 2007. Distribution of Extraterrestrial Chromite in Middle Ordovician Komstad Limestone in the Killeröd Quarry, Scania, Sweden. *Bulletin of the Geological Society of Denmark* 55: 37–58.

Heck, P. R., Schmitz, B., Baur, H., Halliday, A. N., and Wieler, R. 2004. Fast Delivery of Meteorites to Earth after a Major Asteroid Collision. *Nature* 430: 323–25.

Heck, P. R., Schmitz, B., Baur, H., and Wieler, R. 2008. Noble Gases in Fossil Micrometeorites and Meteorites from 470 Myr Old Sediments from Southern Sweden, and New Evidence for the L-Chondrite Parent Body Breakup Event. *Meteoritics & Planetary Science* 43: 517–528.

Heck, P. R., Schmitz, B., Bottke, W. F., Rout, S. S., Kita, N. T., Cronholm, A., Defouilloy, C., Dronov, A., and Terfelt, F. 2017. Rare Meteorites Common in the Ordovician Period. *Nature Astronomy* 1: 35. http://www.nature.com/articles/s41550-016-0035.

Heck, P. R., Schmitz, B., Rout, S. S., Tenner, T., Villalon, K., Cronholm, A., Terfelt, F., and Kita, N. T. 2016. A Search for H-Chondritic Chromite Grains in Sediments that Formed Immediately after the Breakup of the L-Chondrite Parent Body 470 Ma Ago. *Geochimica et Cosmochimica Acta* 177: 120–29.

Heck, P. R., Ushikubo, T., Schmitz, B., Kita, N. T., Spicuzza, M. J., and Valley, J. W. 2010. A Single Asteroidal Source for Extraterrestrial Ordovician Chromite Grains from Sweden and China: High-Precision Oxygen Three-Isotope SIMS Analysis. *Geochimica et Cosmochimica Acta* 74: 497–509.

Herzog, G. F., and Caffee, M. W. 2013. Cosmic-Ray Exposure Ages of Meteorites. edited by A. M. Davis, H. D. Holland and Turekian K. K. *Treatise on Geochemistry*, 2nd ed., 419–454. Oxford: Elsevier Inc.

Jourdan, F., Andreoli, M. A. G., McDonald, I., and Maier, W. D. 2010. ^{40}Ar/^{39}Ar Thermochronology of the Fossil LL6-Chondrite from the Morokweng Crater, South Africa. *Geochimica et Cosmochimica Acta* 74: 1734–47.

Jourdan, F., Kennedy, T., Benedix, G. K., Eroglu, E., and Mayer, C. 2020. Timing of the Magmatic Activity and Upper Crustal Cooling of Differentiated Asteroid 4 Vesta. *Geochimica et Cosmochimica Acta* 273: 205–225.

Kaneoka, I., Ozima, M., and Yanagisawa, M. 1979. ^{40}Ar-^{39}Ar Age Studies of Four Yamato-74 Meteorites. *Memoirs of National Institute of Polar Research*. Special issue, 12: 186–206.

Kennedy, T., Jourdan, F., Eroglu, E., and Mayers, C. 2019. Bombardment History of Asteroid 4 Vesta Recorded by Brecciated Eucrites: Large Impact Event Clusters at 4.50 Ga and Discreet Bombardment until 3.47 Ga. *Geochimica et Cosmochimica Acta* 260: 99–123.

Kita, N. T., Nagahara, H., Tachibana, S., Tomomura, S., Spicuzza, M. J., Fournelle, J. H., and Valley, J. W. 2010. High Precision SIMS Oxygen Three Isotope Study of Chondrules in LL3 Chondrites: Role of Ambient Gas during Chondrule Formation. *Geochimica et Cosmochimica Acta* 74: 6610–35.

Liao, S., and Schmitz, B. 2023. The Mid-Ordovician Meteorite Flux to Earth Shortly Before Breakup of the L-Chondrite Parent Body. *Icarus* 389: 115285.

Lindsay, F. N., Delaney, J. S., Herzog, G. F., Turrin, B. D., Park, J., and Swisher, C. C. 2015. Rheasilvia Provenance

19455100, 0, Downloaded from https://onlinelibrary.wiley.com/doi/10.1111/maps.14133 by Readcube (Labtiva Inc.), Wiley Online Library on [03/02/2024]. See the Terms and Conditions (https://onlinelibrary.wiley.com/terms-and-conditions) on Wiley Online Library for rules of use; OA articles are governed by the applicable Creative Commons License

of the Kapoeta Howardite Inferred from ~1 Ga $^{40}Ar/^{39}Ar$ Feldspar Ages. *Earth and Planetary Science Letters* 413: 208–213.

Lindskog, A., Schmitz, B., Cronholm, A., and Dronov, A. 2012. A Russian Record of a Middle Ordovician Meteorite Shower: Extraterrestrial Chromite at Lynna River, St. Petersburg region. *Meteoritics & Planetary Science* 47: 1274–90.

Lucas, M. P., Emery, J. P., Pinilla-Alonso, N., Lindsay, S. S., and Lorenzi, V. 2017. Hungaria Asteroid Region Telescopic Spectral Survey (HARTSS) I: Stony Asteroids Abundant in the Hungaria Background Population. *Icarus* 291: 268–287.

Malézieux, J., and Piriou, B. 1988. Relation Entre la Composition Chimique et le Comportement Vibrationnel de Spinelles de Synthèse et de Chromites Naturelles en Microspectrométrie Raman. *Bulletin de minéralogie* 111: 649–669.

Marchi, S., McSween, H. Y., O'Brien, D. P., Schenk, P., de Sanctis, M. C., Gaskell, R., Jaumann, R., et al. 2012. The Violent Collisional History of Asteroid 4 Vesta. *Science* 336: 690–94.

Martin, E., Schmitz, B., and Schönlaub, H.-P. 2018. From the Mid-Ordovician into the Late Silurian: Changes in the Micrometeorite Flux after the L Chondrite Parent Breakup. *Meteoritics & Planetary Science* 53: 2541–57.

Marzari, F., Cellino, A., Davis, D. R., Farinella, P., Zappala, V., and Vanzani, V. 1996. Origin and Evolution of the Vesta Asteroid Family. *Astronomy and Astrophysics* 316: 248–262.

Marzari, F., Farinella, P., and Davis, D. R. 1999. Origin, Aging, and Death of Asteroid Families. *Icarus* 142: 63–77.

McGraw, A. M., Reddy, V., and Sanchez, J. A. 2018. Do L Chondrites Come from the Gefion Family? *Monthly Notices of the Royal Astronomical Society* 476: 630–34.

Milani, A., Cellino, A., Knežević, Z., Novaković, B., Spoto, F., and Paolicchi, P. 2014. Asteroid Families Classification: Exploiting Very Large Datasets. *Icarus* 239: 46–73.

Naveen, Sarkar, S., Kumar, T. N., Ray, D., Bhattacharya, S., Shukla, A. D., Moitra, H., Dagar, A., Chauhan, P., Sen, K., and Das, S. 2019. Mineralogy and Spectroscopy (VIS Near Infrared and Micro-Raman) of Chromite from Nidar Ophiolite Complex, SE Ladakh, India: Implications for Future Planetary Exploration. *Planetary and Space Science* 165: 1–9.

Nesvorný, D., Vokrouhlický, D., Bottke, W. F., and Gladman, B. 2007. Express Delivery of Fossil Meteorites from the Inner Asteroid Belt to Sweden. *Icarus* 188: 400–413.

Nesvorný, D., Vokrouhlický, D., Morbidelli, A., Bottke, W. F., and Holešovi˘, V. 2009. Asteroidal Source of L Chondrite Meteorites. *Icarus* 200: 698–701. https://doi.org/10.1016/j.icarus.2008.12.016.

Reddy, B. J., and Frost, R. L. 2005. Spectroscopic Characterization of Chromite from the Moa-Baracoa Ophiolitic Massif, Cuba. *Spectrochimica Acta Part A: Molecular and Biomolecular Spectroscopy* 61: 1721–28.

Roig, F., and Nesvorný, D. 2020. Modeling the Chronologies and Size Distributions of Ceres and Vesta Craters. *The Astronomical Journal* 160: 110.

Rout, S. S., Heck, P. R., and Schmitz, B. 2018. Shock History of the Fossil Ungrouped Achondrite Österplana 065: Raman Spectroscopy and TEM of Relict Chrome-Spinel Grains. *Meteoritics & Planetary Science* 53: 973–983.

Rout, S. S., Heck, P. R., Zaluzec, N. J., Ishii, T., Wen, J., Miller, D. J., and Schmitz, B. 2017. Shocked Chromites in Fossil L Chondrites: A Raman Spectroscopy and Transmission Electron Microscopy Study. *Meteoritics & Planetary Science* 52: 1776–96.

Schenk, P. M., Neesemann, A., Marchi, S., Otto, K., Hoogenboom, T., O'Brien, D. P., Castillo-Rogez, J., Raymond, C. A., and Russell, C. T. 2022. A Young Age of Formation of Rheasilvia Basin on Vesta from Floor Deformation Patterns and Crater Counts. *Meteoritics & Planetary Science* 57: 22–47.

Schmedemann, N., Kneissl, T., Ivanov, B. A., Michael, G. G., Wagner, R. J., Neukum, G., Ruesch, O., et al. 2014. The Cratering Record, Chronology and Surface Ages of (4) Vesta in Comparison to Smaller Asteroids and the Ages of HED Meteorites. *Planetary and Space Science* 103: 104–130.

Schmitz, B. 2013. Extraterrestrial Spinels and the Astronomical Perspective on Earth's Geological Record and Evolution of Life. *Chemie der Erde* 73: 117–145.

Schmitz, B., Farley, K. A., Goderis, S., Heck, P. R., Bergström, S. M., Boschi, S., Claeys, P., et al. 2019. An Extraterrestrial Trigger for the Mid-Ordovician Ice Age: Dust from the Breakup of the L-Chondrite Parent Body. *Science Advances* 5: eaax4184.

Schmitz, B., Feist, R., Meier, M. M. M., Martin, E., Heck, P. R., Lenaz, D., Topa, D., et al. 2019. The Micrometeorite Flux to Earth during the Frasnian–Famennian Transition Reconstructed in the Coumiac GSSP Section, France. *Earth and Planetary Science Letters* 522: 234–243.

Schmitz, B., Häggström, T., and Tassinari, M. 2003. Sediment-Dispersed Extraterrestrial Chromite Traces a Major Asteroid Disruption Event. *Science* 300: 961–64.

Schmitz, B., Heck, P. R., Alvarez, W., Kita, N. T., Rout, S. S., Cronholm, A., Defouilloy, C., et al. 2017. Meteorite Flux to Earth in the Early Cretaceous as Reconstructed from Sediment-Dispersed Extraterrestrial Spinels. *Geology* 45: 807–810.

Schmitz, B., Huss, G. R., Meier, M. M. M., Peucker-Ehrenbrink, B., Church, R. P., Cronholm, A., Davies, M. B., et al. 2014. A Fossil Winonaite-Like Meteorite in Ordovician Limestone: A Piece of the Impactor that Broke up the L-Chondrite Parent Body? *Earth and Planetary Science Letters* 400: 145–152.

Schmitz, B., Tassinari, M., and Peucker-Ehrenbrink, B. 2001. A Rain of Ordinary Chondritic Meteorites in the Early Ordovician. *Earth and Planetary Science Letters* 194: 1–15.

Schmitz, B., Yin, Q.-Z., Sanborn, M. E., Tassinari, M., Caplan, C. E., and Huss, G. R. 2016. A New Type of Solar-System Material Recovered from Ordovician Marine Limestone. *Nature Communications* 7: ncomms11851.

Suavet, C., Alexandre, A., Franchi, I. A., Gattacceca, J., Sonzogni, C., Greenwood, R. C., Folco, L., and Rochette, P. 2010. Identification of the Parent Bodies of Micrometeorites with High-Precision Oxygen Isotope Ratios. *Earth and Planetary Science Letters* 293: 313–320.

Suttle, M. D., Dionnet, Z., Franchi, I., Folco, L., Gibson, J., Greenwood, R. C., Rotundi, A., King, A., and Russell, S. S. 2020. Isotopic and Textural Analysis of Giant Unmelted Micrometeorites—Identification of New Material from Intensely Altered ^{16}O-Poor Water-Rich Asteroids. *Earth and Planetary Science Letters* 546: 116444.

Terfelt, F., and Schmitz, B. 2021. Asteroid Break-Ups and Meteorite Delivery to Earth the Past 500 Million Years.

19455100, 0, Downloaded from https://onlinelibrary.wiley.com/doi/10.1111/maps.14133 by Readcube (Labtiva Inc.), Wiley Online Library on [03/02/2024]. See the Terms and Conditions (https://onlinelibrary.wiley.com/terms-and-conditions) on Wiley Online Library for rules of use; OA articles are governed by the applicable Creative Commons License

Proceedings of the National Academy of Sciences of the United States of America 118, e2020977118.
Tuschel, D. 2015. The Correlation Method for the Determination of Spectroscopically Active Vibrational Modes in Crystals. *Spectroscopy* 30: 17–22.
Vernazza, P., Zanda, B., Binzel, R. P., Hiroi, T., DeMeo, F. E., Birlan, M., Hewins, R., Ricci, L., Barge, P., and Lockhart, M. 2014. Multiple and Fast: The Accretion of Ordinary Chondrite Parent Bodies. *The Astrophysical Journal* 791: 120.
Wang, A., Kuebler, K. E., Jolliff, B. L., and Haskin, L. A. 2004. Raman Spectroscopy of Fe-Ti-Cr-Oxides, Case Study: Martian Meteorite EETA79001. *American Mineralogist* 89: 665–680.
Wojdyr, M. 2010. Fityk: A General-Purpose Peak Fitting Program. *Journal of Applied Crystallography* 43: 1126–28.

SUPPORTING INFORMATION

Additional supporting information may be found in the online version of this article.

Table S1. Overview of classification system from Heck et al. (2017) based on O-isotopes and elemental oxides and Terfelt and Schmitz (2021) based on elemental oxides only. TFL=Terrestrial Mass Fractionation Line in three oxygen isotope space.

Table S2. Complete data table.

Figure S1. Comparison of the chrome-spinel classification based on $\Delta^{17}O$ and TiO_2 and of the one based on elemental concentrations only. HED, Howardite–eucrite–diogenite clan. Other abbreviations as defined in Terfelt and Schmitz (2022): "EC" = extraterrestrial chrome spinel; "OtC" = Other chrome spinel; V-rich "OtC" grains.

Figure S2. Correlation of major cation (Cr^{3+}, Fe^{3+}) occupancy of octahedral sites versus the A1g (v1) mode. All data points are shown.

Figure S3. Raman spectra of samples from the different classes defined in Heck et al. (2017).

Figure S4. Cross plots of prominent A1g Raman peak and minor and major oxide concentrations. All data points are shown.

19455100, 0, Downloaded from https://onlinelibrary.wiley.com/doi/10.1111/maps.14133 by Readcube (Labtiva Inc.), Wiley Online Library on [03/02/2024]. See the Terms and Conditions (https://onlinelibrary.wiley.com/terms-and-conditions) on Wiley Online Library for rules of use; OA articles are governed by the applicable Creative Commons License